For publication in ***Ocean Dynamics***

Evaluation of wave model performance in the South Atlantic Ocean: a study about physical parameterization and wind forcing calibration

Júlia Kaiser[1*] · Izabel C.M. Nogueira[1] · Ricardo M. Campos[2,3] · Carlos E. Parente[1] Renato P. Martins[4] · Wellington C. Belo[4]

Conflict of interest

The authors declare that they have no conflict of interest.

Abstract This paper evaluates the performance of the spectral wave model WAVEWATCH III for the South Atlantic Ocean forced by wind inputs from the most recent reanalyses, NCEP/CFSR and ECMWF/ERA5, combined with two different source terms: ST4 and ST6. A calibration is performed considering one year (2012) and 31 simulations, evaluated against altimeter and buoy data through six error metrics and Q-Q plots. Assessment results suggest that both ST4 and ST6 provide good results when WAVEWATCH III is properly adjusted for the wind input. Nevertheless, the wave model presents a positive bias of significant wave height when forced by CFSR winds that requires attention. The investigation in the spectral domain indicates a better performance of wave simulations forced by ERA5 winds, especially for wave periods below 10 s. For wave periods above 10 s, the choice of source-term package becomes more important. In this regard, ST4 parameterization combined with ERA5 winds presents the best results for the region. The optimal range of calibration parameters for each wind input and source term package is reported and discussed.

Júlia Kaiser (*corresponding author)
E-mail: js.kaiser@oceanica.ufrj.br

[1] Ocean Engineering Program, Federal University of Rio de Janeiro, Rio de Janeiro, Brazil

[2] Cooperative Institute for Marine and Atmospheric Studies (CIMAS), 4600 Rickenbacker Causeway, University of Miami, Miami, FL 33149, USA

[3] NOAA/Atlantic Oceanographic and Meteorological Laboratory (AOML), 4301 Rickenbacker Causeway, Miami, FL 33149, USA

[4] Centro de Pesquisas e Desenvolvimento Leopoldo A. Miguez de Mello, Petróleo Brasileiro, Rio de Janeiro, Brazil

Keywords wave modeling · wave hindcast · WAVEWATCH III · source terms · wind forcing fields · South Atlantic Ocean

Acknowledgements The authors would like to thank the Brazilian National Buoy Program (PNBOIA) of the Brazilian Navy for providing the wave data, and the Federal University of Rio de Janeiro through Laboratório de Instrumentação Oceanográfica for all the technical and scientific support. The authors acknowledge Petrobras for the collaboration and ANP (Agência Nacional de Petróleo, Gás Natural e Biocombustíveis) for the research fund. The third author has been funded by the Cooperative Institute for Marine and Atmospheric Studies (CIMAS), a Cooperative Institute of the University of Miami and the National Oceanic and Atmospheric Administration, cooperative agreement NA20OAR4320472.

1 Introduction

Wave hindcasts are essential tools to study the sea state pattern especially in regions where observational data are scarce. The South Atlantic Ocean, in particular, is known by its lack of in situ measurements (Cuchiara et al., 2009; Pianca et al., 2010; Chawla et al., 2013) and most of the buoy dataset in the region is recent (Pereira et al., 2017). This lack of observations severely compromises the wave climate studies since it can only be determined if the data period considered is large enough to cover both seasonal and inter-annual variability as well as long term wave characteristics (Young, 1999). In that sense, numerical wave models become a particularly interesting tool to investigate the sea state pattern in the region (Alves et al., 2009; Pianca et al., 2010; Innocentini et al., 2014; Campos et al., 2018).

Using model results, Pianca et al. (2010) show the wave climate in the southern and southeastern sectors of the Brazilian Continental Shelf is controlled by the South Atlantic High and the passage of synoptic cold fronts. The waves in the south and southeastern Brazilian coast present extreme values that reach up to 7 m (Parente, 1999; Campos et al., 2012; Godoi et al., 2014; Campos and Guedes Soares, 2016b; Pianca et al., 2010). The eastern, northeastern and northern sectors have a wave climate mostly affected by the Intertropical Convergence Zone and its meridional oscillation. Most of the Brazilian coast is highlighted by the multimodal sea states characteristics (Violante-Carvalho et al., 2002; Pianca et al., 2010; Semedo et al., 2011). In general, the wave energy decreases from south to north (Pianca et al., 2010; Pereira et al., 2017) with a predominance of more than 85% of Hs values below 3 m and the dominance of Tp classes of 6-8 and 10-12 s (Pereira et al., 2017) in the southernmost area. The northeast portion of the Brazilian coast is characterized the predominant wave energy coming from the east quadrant most of the year with a mean significant wave height between 1 to 2 m during the spring and summer seasons and between 2 and 3 m during fall and winter (Pianca et al., 2010).

In the last 30 years, there have been great advances in the physical parameterizations of the third generation wave models, such as WAVEWATCH III (WW3DG, 2019), hereinafter WW3. In this case, the source term that governs the balance between wind input and wave dissipation has been highlighted. It is well know that in deep waters these are two of the main process that control the characteristics of the wave field.

Stopa et al. (2016) made a meticulous study of inter-comparing the performance of the four available parameterizations packages in WW3: ST2 (or TC96) (Tolman and Chalikov, 1996), ST3 (WAM4+) (Bidlot et al., 2007; Janssen, 1991), ST4 (Ardhuin et al., 2010), and ST6 (or BYDRZ) (Zieger et al., 2015). All the simulations were made for the year 2011 at global scale with CFSR (Saha et al., 2014) as wind forcing field. Altimeter, buoy, and SAR data were considered for the comparisons. The results found by Stopa et al. (2016) show that ST4 and ST6 packages performs similarly and both packages suit better to data than ST2 and ST3. While ST4 package has the lowest significant wave height biases, ST6 package generally produces more accurate swell heights. Recently, Liu et al. (2019) recalibrated the configurations of the ST6 package, improving the modeling performance considering a series of academic and realistic simulations. Despite the aforementioned studies, there is still little effort to validate these packages for the South Atlantic Ocean specifically.

Furthermore, considering the growing number of wind products (Kalnay et al., 1996; Dee et al., 2011; Rienecker et al., 2011; Saha et al., 2014; Kobayashi et al., 2015; Hersbach et al., 2020), it is important to understand the differences found in the wave field when using different source term packages considering distinct wind datasets as input. Stopa (2018) presented a calibration study, performed globally, using the ST4 package on WW3 considering 12 different wind inputs for the year of 2001. With different values of wind to wave growth parameter, Stopa (2018) was able to calibrate the model and all of them reproduces the average sea states similarly. However, considerable differences were found for in sea state conditions of high energy. Stopa (2018) shows that the reanalysis CFSR (Saha et al., 2014), ERAI (Dee et al., 2011), JRA55 (Kobayashi et al., 2015) and MERRA (Rienecker et al., 2011) are better forcing wind fields for wave hindcasting and ERAI is highlighted as one of the most precise reanalysis with the lowest scatter index of wave parameters.

With the recent release of ERA5 reanalysis by the European Centre for Medium-Range Weather Forecasts (ECMWF) (Hersbach et al., 2020) as the ERAI successor, the aim of this work is to evaluate the performance of the spectral wave model WW3 for the South Atlantic area considering ST4 and ST6 source terms using the two most recent reanalyses as wind input: CFSR and ERA5. The remainder is organized as follows. Section 2 addresses details about the model and the source terms. Section 3 presents the wind field characteristics from CFSR and ERA5 databases. Section 4 describes the methodology applied to calibrate and validate the wave model, using altimeter and buoy data for the year of 2012. In section 5 the spatial statistics are presented while the in-situ analysis is presented in section 6. Discussions and conclusions follow in section 7.

2 Wave model

The wave hindcasts are generated using WAVEWATCH III version 6.07 (WW3DG, 2019). The WW3 model was run for two different grids: Grid 1 covered the Atlantic Ocean and part of the Pacific Ocean, while grid 2 covered the Southern Atlantic Ocean – grid details can be found in Table 1. The bathymetric data used is part of the ETOPO1 database from NOAA Amante and Eakins (2009). The model was

implemented with a spectral resolution of 36 directions and 35 logarithmically spaced frequencies, between 0.0377 Hz (26.5 s) and 0.963 Hz (1.0 s).

Table 1 Main characteristics of the grids used to generate wave hindcasts. $\Delta_{x,y}$ is the spatial resolution of the grids in degrees; N_x and N_y are the numbers of points in x and y, respectively; Lat_i is the initial latitude, Lon_i is the initial longitude, Lat_f is the final latitude, and Lon_f is the final longitude of the grids.

	Grid 1	**Grid 2**
$\Delta_{x,y}$	1°	0.25°
N_x	111	121
N_y	141	161
Lat_i	-80°	-45°
Lon_i	-90°	-65°
Lat_f	60°	-5°
Lon_f	20°	-10°

WW3 integrates the spectral wave action equation in space and time, with discretized wave numbers and directions. Conservative wave processes, represented by the local rate of change and spatial and spectral transport terms are balanced by the non-conservative sources and sinks. For deep water it is generally accepted that the total source/sinks term is based on three main physical processes: atmospheric input S_{in}, wave dissipation S_{ds}, and wave-wave nonlinear interactions S_{nl} (Komen et al., 1984; Ardhuin et al., 2010; Zieger et al., 2015).

As explained in the model manual (WW3DG, 2019), although S_{in} and S_{ds} represent separate processes, they are related to each other since the balance between these two source terms governs the integral growth characteristics of the wave energy. WW3 includes various source term packages (or physics) that describe the wind input and dissipation: ST1 (or WAM3) (Komen et al., 1984), ST2 (or TC96) (Tolman and Chalikov, 1996), ST3 (WAM4+) (Bidlot et al., 2007; Janssen, 1991), and recent implementations of ST4 (Ardhuin et al., 2010), and ST6 (or BYDRZ) (Zieger et al., 2015).

The ST4 parameterization is described by Ardhuin et al. (2010) and uses a positive part of the wind input that is taken from WAM4, with modified friction velocity to balance saturation-based dissipation. The dissipation term is defined as the sum of the saturation-based term, the cumulative breaking term and the wave-turbulence interaction term (Ardhuin et al., 2009). Depending on the quality of the wind field, a wind-wave growth parameter β_{max} can be adjusted.

The ST6 or Babanin/Young/Donelan/Rogers/Zieger (BYDRZ) (Zieger et al., 2015) is largely inspired from the energy balance determined from the Lake George measurements presented by Young et al. (2005). This scheme implements observation-based physics for deep-water source/sink terms and includes negative wind input, whitecapping dissipation, and wave-turbulence interactions (swell dissipation). In ST6, bulk adjustment to the wind field can be achieved by re-scaling the drag parameterization through the parameter FAC. This has a similar effect to tuning the parameter β_{max} in ST4 source term package.

In this work, we modify β_{max} and FAC to determine the optimum point considering different significant wave height error indexes and to reduce the bias according to the wind field used as input. The main features of each simulation are summarized in Table 2 and all of them were made for the year of 2012.

Table 2 Main features of WW3 simulations.

ID	INPUT	PHYSICS	β_{MAX}/FAC
T101	CFSR	ST4	1.25
T102	CFSR	ST4	1.33
T103	CFSR	ST4	1.385
T104	CFSR	ST4	1.437
T105	CFSR	ST4	1.46
T106	CFSR	ST4	1.50
T107	CFSR	ST4	1.55
T108	CFSR	ST4	1.60
T109	CFSR	ST4	1.65
T112	CFSR	ST6	1.00
T113	CFSR	ST6	1.10
T114	CFSR	ST6	1.15
T115	CFSR	ST6	1.18
T116	CFSR	ST6	1.23
T117	CFSR	ST6	1.28
T118	CFSR	ST6	1.33
T201	ERA5	ST4	1.33
T202	ERA5	ST4	1.55
T203	ERA5	ST4	1.70
T204	ERA5	ST4	1.80
T205	ERA5	ST4	1.85
T206	ERA5	ST4	1.90
T207	ERA5	ST4	2.00
T208	ERA5	ST4	2.10
T212	ERA5	ST6	1.00
T213	ERA5	ST6	1.23
T214	ERA5	ST6	1.26
T215	ERA5	ST6	1.29
T216	ERA5	ST6	1.33
T217	ERA5	ST6	1.40
T218	ERA5	ST6	1.50

3 Forcing wind fields

The CFSR (Climate Forecast System Reanalysis) is a third generation reanalysis product from the National Centers for Environmental Prediction (NCEP), with global coverage. It includes a 6-hourly coupling between the atmosphere and ocean, an interactive sea ice model and higher spatial and temporal model outputs (Saha et al., 2014). The wind product from CFSR refers to 10-meters winds on the T382 grid with a grid spacing of $0.31^\circ \times 0.31^\circ$ in the tropics and hourly temporal resolution output. The version 2 of CFSR was released in March 2011 and is operational since then. There are many papers that verify the good performance of wave hindcasts using the CFSR wind data as an input (Chawla et al., 2013; Stopa and Cheung, 2014; Stopa et al., 2016; Campos and Guedes Soares, 2016a).

The European Centre for Medium Range Weather Forecast ReAnalysis 5 (ERA5) is the most recent atmospheric reanalyses of the global climate produced by ECMWF. It was completely made available for public use in January 2019 and provide hourly estimates of a large number of atmospheric, land, and oceanic variables since 1950 until the present. ERA5 has spacial resolution of 31 km for wind products and replaces the renowned ERA-Interim reanalysis that was launched by ECMWF in 2006 and has spatial resolution of 79 km.

4 Observations

4.1 Altimeter

Significant wave height data from the Ifremer Merged Altimeter Database was used in order to calibrate and spatially validate the WW3 simulations. Through GlobWave project, this database is made available by CERSAT group and all data are quality controlled by Queffeulou and Croizé-Fillon (2017). In that sense, the methodology applied to evaluate the wave hindcast according to altimeter data is based on the collocation model results according to satellite tracks for the year of 2012. Since the purpose of this work is to evaluate the overall error statistics on South Atlantic scale, only points with a match between valid model results and altimeter data located far from the coastlines and in areas where the depth is greater than 70 m were considered.

The error metrics correlation coefficient (R), root mean square error (RMSE), bias (BIAS), and the scatter index (SI) were used according to equations 1 to 6 to access the quality of the model estimates (y - model, x - observations). When this kind of analysis is performed with spatially distributed data, it is possible to visualize the map distribution of the error statistics and identify areas where model inaccuracies grow.

$$R = \frac{\sum_{i=1}^{n}(x_i - \bar{x})(y_i - \bar{y})}{\sqrt{\sum_{i=1}^{n}(x_i - \bar{x})^2 \sum_{i=1}^{n}(y_i - \bar{y})^2}} \tag{1}$$

$$BIAS = \frac{\sum_{i=1}^{n}(y_i - x_i)}{n} \tag{2}$$

$$NBIAS = \frac{\frac{\sum_{i=1}^{n}(y_i - x_i)}{n}}{\sqrt{\frac{\sum_{i=1}^{n} x_i^2}{n}}} \tag{3}$$

$$RMSE = \sqrt{\frac{\sum_{i=1}^{n}(y_i - x_i)^2}{n}} \tag{4}$$

$$NRMSE = \sqrt{\frac{\sum_{i=1}^{n}(y_i - x_i)^2}{\sum_{i=1}^{n}(x_i)^2}} \tag{5}$$

$$SI = \frac{\sqrt{\frac{1}{n}\sum_{i=1}^{n}[(y_i - \bar{y}) - (x_i - \bar{x})]^2}}{\bar{x}} \tag{6}$$

4.2 Buoys

In order to validate the WW3 simulations using both the significant wave height (Hs) and also the spectral data, hourly observations from four buoys maintained by the Brazilian Navy through the Brazilian National Program (PNBOIA) were used (Fig. 1). Detailed information about the buoys are presented by Pereira et al. (2017) and duration of each buoy dataset considered here is presented in figure 2. Despite the short duration of buoy observations, the heave-pitch-roll buoy records of wave spectra allow a deeper investigation of the wave model performance in the spectral domain.

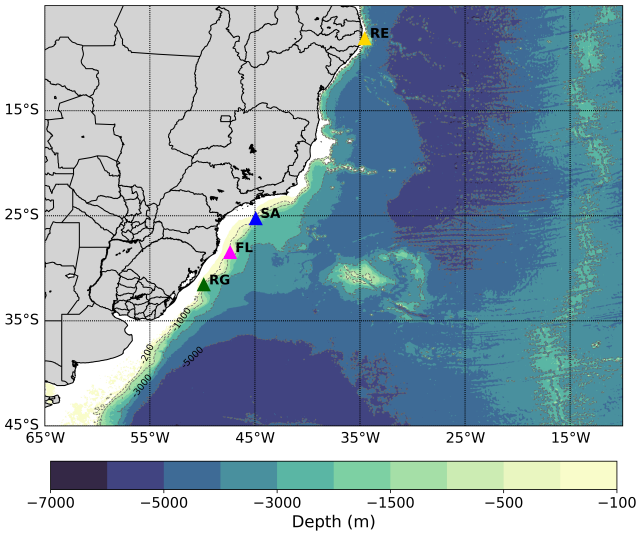

Fig. 1 Location of the four buoys used to calibrate and validate WW3 simulations. The area of the map coincides with Grid 2 employed in the wave model. More information about model grids coverage can be found in Table 1.

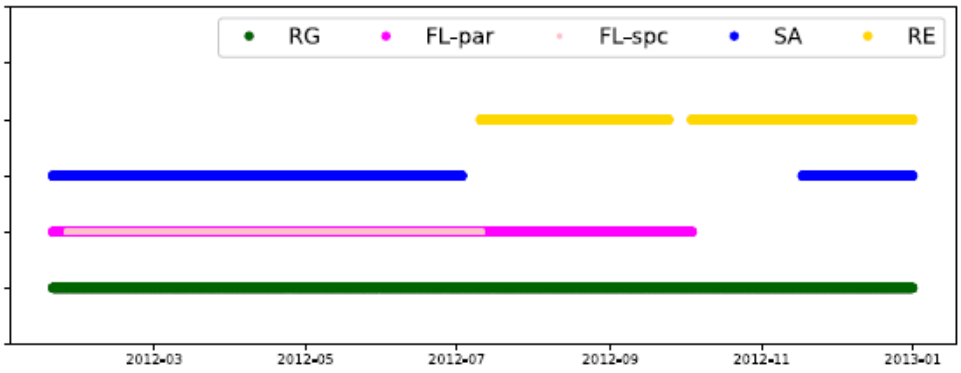

Fig. 2 Temporal availability of wave buoys dataset. For RG and SA buoys the colored lines refers to both, bulk parameters and wave spectra records availability. For FL buoy, magenta line refers to bulk parameters (FL-par) while light pink line refers to wave spectra records (FL-spc). For RE buoy, the yellow line refers to wave bulk parameters availability.

The same typical error metrics is used to evaluate the WW3 simulations punctually - R, RMSE, BIAS, and SI. The normalized metrics (NBIAS and NRMSE, respectively from equations 3 and 5) are also calculated, mainly for the spectral analysis. In that sense, section 6.2 evaluate the performance of the different simulations in representing the energy distribution along the spectra through the analysis of wave height in four different frequency classes. The number of wave records of each buoy is shown in Table 3. The spectral data of RE buoy did not show consistency, and therefore will not be considered in the analyzes.

Table 3 Number of observations (wave spectra and integral parameters) retrieved from buoys RG, FL, SA and RE.

Buoy	Position	Depth	Wave spectra	Bulk parameters
RG	31.566°S / 49.966°W	200 m	8297	8297
FL	28.500°S / 47.366°W	200 m	3979	6190
SA	25.283°S / 44.933°W	200 m	4998	4998
RE	8.149°S / 34.560°W	200 m	-	3950

5 Wave field statistics

From the Quantile-Quantile (Q-Q) plots for altimeter data (Fig. 3), it is clear that larger values of β_{max} and FAC result in higher wave heights. It means updates of β_{max} or FAC can be used to deal with some energy underestimation or overestimation faced in WW3 simulations. In the Q-Q plots, the better the simulation the closer it should be to the main diagonal representing the line of perfect agreement (in black). This situation only happens when the model performs well from calm to extreme wave conditions. Comparing the WW3 simulations forced by CFSR and ERA5 winds, for the same β_{max} in ST4 (T102 and T201, for example), it is observed that those with CFSR input result in higher values of Hs values. The same behavior is observed by taking the simulations with ST6 and fixing the FAC value. The positive bias of the CFSR winds and its impact on the positive bias of the Hs has already been reported in Chawla et al. (2013); Stopa and Cheung (2014); Rapizo et al. (2018). In terms of quantiles, the best results with CFSR are obtained with the lowest values of β_{max} and FAC (T101 and T112, respectively). Regarding simulations with ERA5 as input, the simulation T203 is especially highlighted for its best match with altimeter data considering the total area of Grid 2.

Figures 4 and 5 show the calibration of β_{max} and FAC to determine the optimal values to calibrate the model and reduce RMSE and BIAS of Hs, respectively. The dark colors (dark blue and dark pink) show the results of the comparison between altimeter data and the model runs for the entire area of Grid 2 while the light colors (light blue and light pink) indicate the results obtained by comparing the simulations with the observations of the four buoys together.

Figure 4 alone indicates that model simulations using ST4 parameterization (top panels) present less variable results for RMSE. Considering WW3 simulation forced by ERA5 winds, the lowest RMSE of Hs is associated with test T202 (ST4 with β_{max}=1.55) when compared to the altimeter data and T203 (ST4 with

β_{max}=1.70) when compared with buoys data. In terms of BIAS, the simulation T202 (ST4 with β_{max}=1.55) presents better results when compared to altimeter database and T213 (ST6 with FAC=1.23) is highlighted when compared to the buoys time series. When the results obtained using CFSR as input are analyzed, four simulations have lower errors in terms of RMSE and BIAS: T101 (ST4 with β_{max}=1.25), T103 (ST4 with β_{max}=1.385), T112 (ST6 with FAC=1.0), and T113 (ST6 with FAC=1.1).

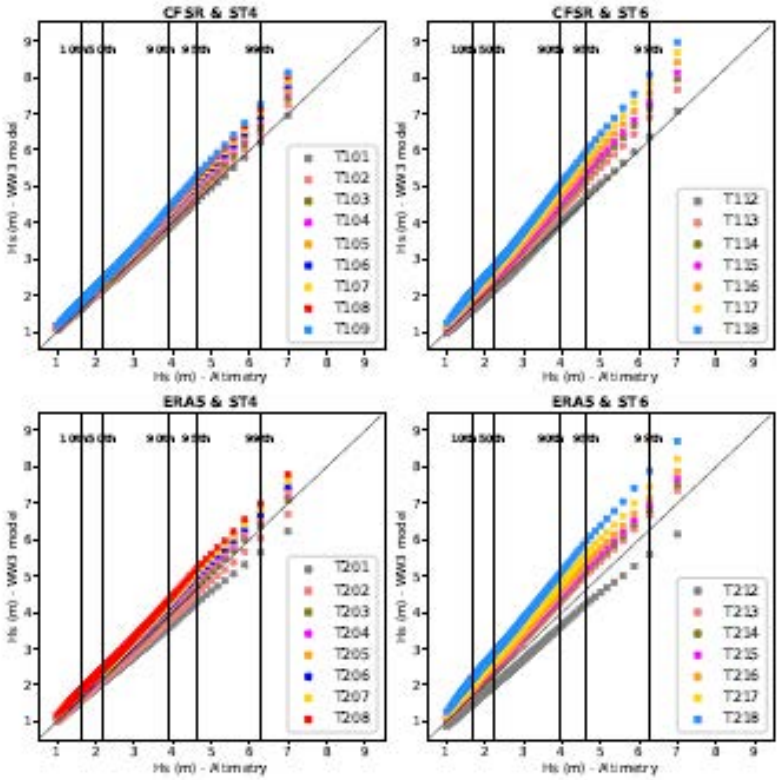

Fig. 3 Quantile-Quantile plots created by changing the parameters β_{max} (left panels) and FAC (right panels) and using CFSR (top panels) and ERA5 (bottom panels) winds as input. The colors denote different wave hindcasts according to Table 2.

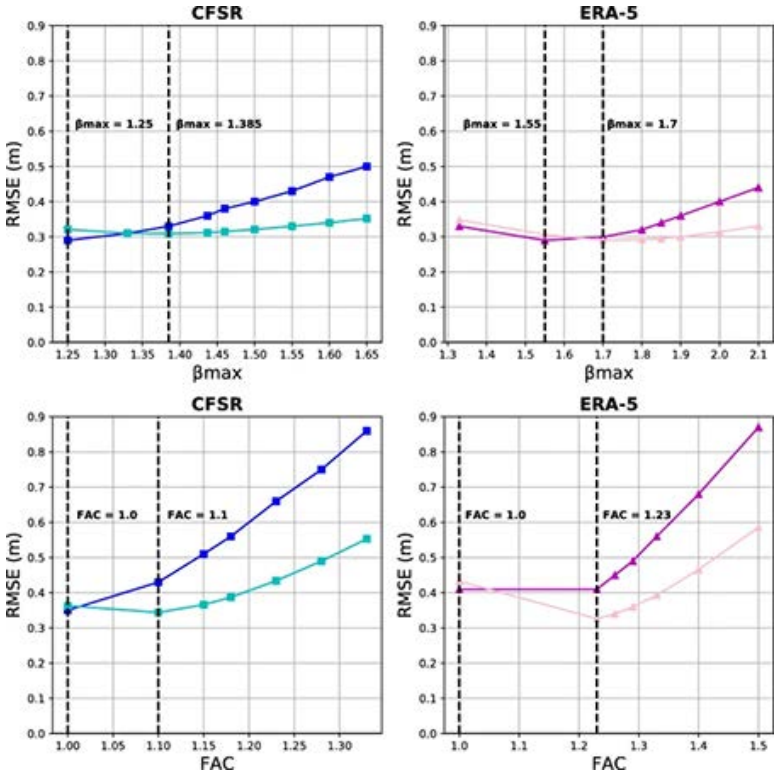

Fig. 4 Calibration of the forcing wind fields (CFSR x ERA5) by modifying β_{max} and FAC according to altimeter wave height (dark blue and dark pink) and to the combined four wave buoy records (light blue and light pink). The β_{max} and FAC values with best results for RMSE are specified by the vertical black line.

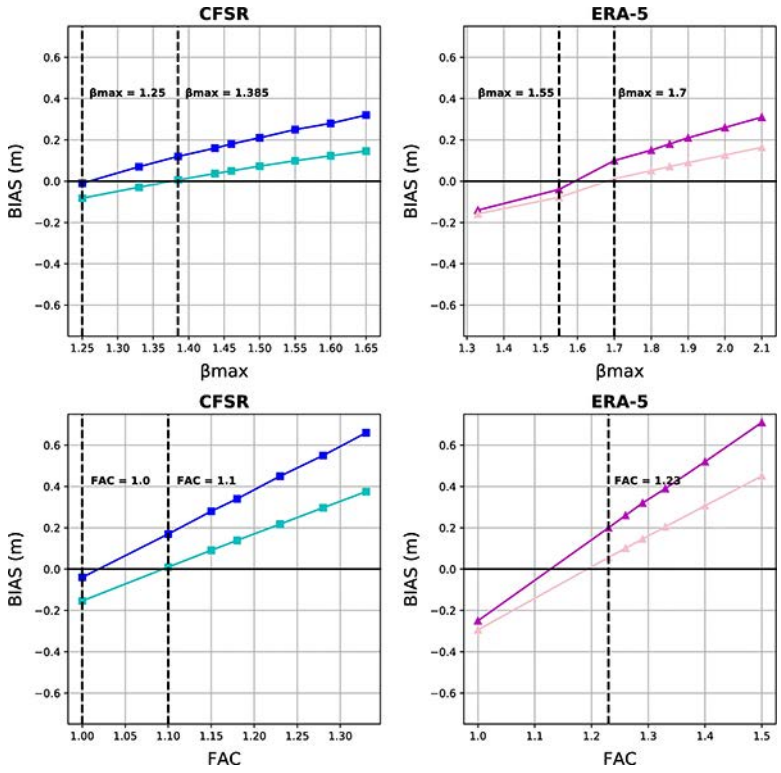

Fig. 5 Calibration of the forcing wind fields (CFSR x ERA5) by modifying β_{max} and FAC according to altimeter wave height (dark blue and dark pink) and to the combined four wave buoy records (light blue and light pink). The β_{max}/FAC values with best results for BIAS are specified by the vertical black line.

6 Comparison with Buoys

6.1 Bulk parameters

A total of 23435 of pairs model/observations were selected for the bulk parameters analysis. As already mentioned, figures 4 and 5 show the calibration of β_{max} and FAC considering the four buoys together (light colors). The results of the calibration using information from the buoys behave very similarly to that presented for altimeters. Thus, in the following analyzes, the simulations that showed the best adjustment to the observational data (altimeters and buoys) will be emphasized: T101, T103, T112, T113, T202, T203, and T213.

Figure 6 shows the Taylor Diagram for the referred simulations. As also observed in Zieger et al. (2015), in general, both ST4 and ST6 show good results when adjusted for the wind. Even though, the best correlation coefficient (R) in terms of Hs has been found in T203 (ST4 with β_{max}=1.70 and ERA5 as wind input), providing also the lowest RMSE (0.29 m) and the lowest scatter index (14.5%). The best adjustment found using ST6 was T213 (ST6 with FAC=1.23 and ERA5 as input), which presents a scatter index of 16.8% and the correlation coefficient of 0.90. The error metrics of these seven simulations for the Hs, peak period (Tp), and peak direction (Dp) are summarized in Table 4.

With respect to Tp, the lowest SI was obtained with ST4 package using ERA5 as input with β_{max}=1.55 (test T202), which is a simulation with general performance very similar to T203). In terms of Dp, the best correlation coefficient and also the lowest SI was obtained for simulation T213 (ST6) with FAC=1.23 and ERA5 as input. Since Tp and Dp are not integral parameters but relate to the spectral peak, the error metrics for Tp and Dp are not as robust as the results for Hs. However, the magnitude of the errors of these parameters (especially for Tp, which is near to 2 s in all cases) do not compromise the results of the spectral analyzes presented below.

Table 4 Statistical results for the wave parameters significant wave height (Hs), peak period (Tp) and peak direction (Dp) considering the seven hindcasts evaluated for the buoys sites.

	T101	**T103**	**T112**	**T113**	**T202**	**T203**	**T213**
R - Hs	0.90	0.90	0.89	0.88	0.91	0.92	0.90
BIAS - Hs (m)	-0.08	0.01	-0.15	0.01	-0.08	0.01	0.06
NBIAS - Hs (%)	-3.9	0.3	-7.3	0.5	-3.7	0.6	2.7
RMSE - Hs (m)	0.32	0.31	0.36	0.34	0.31	0.29	0.33
NRMSE - Hs (%)	15.1	14.6	17.1	16.2	14.5	13.6	15.4
SI - Hs (%)	15.5	15.5	16.5	17.2	14.9	14.5	16.8
R - Tp	0.61	0.60	0.66	0.64	0.65	0.64	0.66
BIAS - Tp (s)	0.28	0.53	0.39	0.72	-0.11	0.23	0.52
NBIAS - Tp (%)	2.9	5.5	4.1	7.6	-1.2	2.4	5.4
RMSE - Tp (s)	2.02	2.13	1.98	2.13	1.83	1.90	1.95
NRMSE - Tp (%)	21.2	22.3	20.7	22.3	19.1	19.9	20.4
SI - Tp (%)	21.6	22.3	20.9	21.7	19.7	20.4	20.3
R - Dp	0.66	0.66	0.70	0.70	0.72	0.72	0.76
BIAS - Dp (°)	6.62	7.17	3.32	2.93	1.32	2.92	-2.17
NBIAS - Dp (%)	4.7	5.1	2.4	2.1	0.9	2.1	-1.5
RMSE - Dp (°)	45.67	45.53	42.86	42.52	40.82	41.22	38.17
NRMSE - Dp (%)	32.4	32.3	30.4	30.2	28.9	29.3	26.8
SI - Dp (%)	35.0	34.9	33.1	32.9	31.6	31.8	29.6

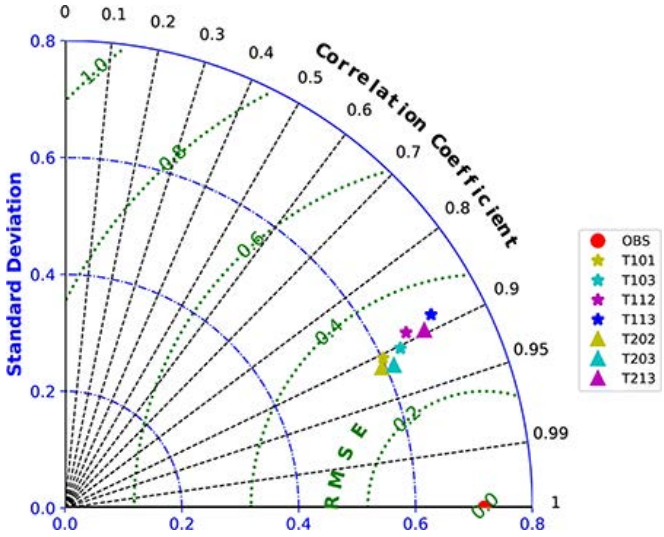

Fig. 6 Taylor diagram comparing the significant wave height from the observation (OBS - red dot) and the seven wave hindcasts results (stars and triangles) considering the time series of the four buoys together.

6.2 Spectral analysis

In this section the simulations were analyzed considering the information on the frequency wave spectrum. Frequency bands with intervals of 0.25 Hz (4 s) were selected and the wave height associated with each band was calculated. This analysis comprised waves with frequency from 0.5 Hz (2 s) up to the upper limit of around 0.0556 Hz (precisely 18 s). For the spectral analysis, the information of the three southernmost buoys was considered separately. Figures 7, 8, and 9 presents the SI, NBIAS, and NRMSE results for RG, FL, and SA buoys, respectively. The dashed lines in the figures represent the simulations with best adjustment to the observational bulk parameters (the already mentioned T101, T103, T112, T113, T202, T203, and T213). When looking at the metrics together, it can be seen the seven tests presents a good agreement with observational data in the frequency analysis – with emphasis on the T202 and T203 tests.

In general, there is a tendency of increase the error values towards the classes of longer periods (low frequency waves). As pointed by Babanin and Jiang (2017), despite the efforts to include new parameterizations for swell dissipation, third generation models still encounter problems to well reproduce longer waves. In global simulations, Babanin and Jiang (2017) affirms that errors associated with the swell height reproduction are two or more times greater than those related to integrated wave height. An increase in the variability of error values is also observed as the wave period increases, which suggests that the choice of the optimal β_{max}/FAC value is more sensitive in longer period waves.

Looking to the results for the waves with period less than 10 s, it seems the performance of the model simulations is more affected by the choice of the wind input product than the physical parameterization. In these period classes, both parameterization (ST4 and ST6) present good results, with most simulations showing SI between 20-25% in the three buoys. On the other hand, better results are obtained with simulations made using wind field from ERA5. This pattern is more evident for buoys FL and RG, which are located closer to the main wave generation areas of the South Atlantic (Reboita et al., 2010; Gramcianinov et al., 2020a,b).

For waves in the last two classes (periods greater than 10 s), the choice of source-term package becomes more important. The errors obtained using ST6 are greater than ST4 with additional large variation when FAC is modified. The simulations with ST4 and ERA5 must be highlighted due to its good performances, with SI and NRMSE respectively below 35% and 30% for the waves with periods between 10 and 14 s for all the three points analyzed. With this same configurations, the model performance for the waves of the last period class (14 to 18 s) showed NBIAS varying from negative to positive values but always less than 30% for RG site and less than 20% for FL and SA.

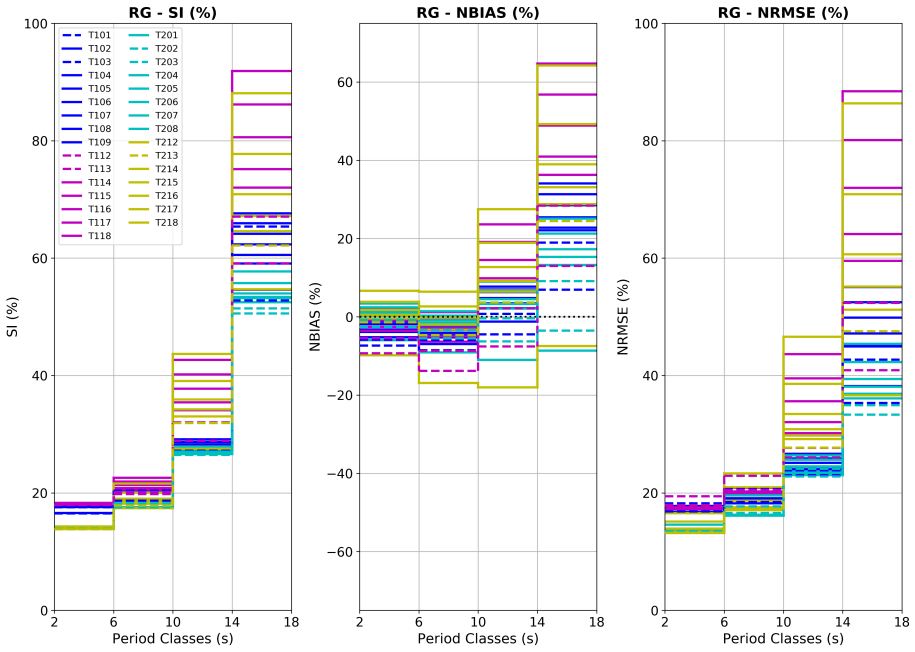

Fig. 7 Results of Hs Scatter Index (SI - left panel), Hs normalized bias (NBIAS - middle panel), and HS normalized RMSE (NRMZE - right panel) of buoy RG distributed over the classes of wave period. The dashed lines indicate the simulations with best adjustment to the observational bulk parameters: T101, T103, T112, T113, T202, T203, and T213.

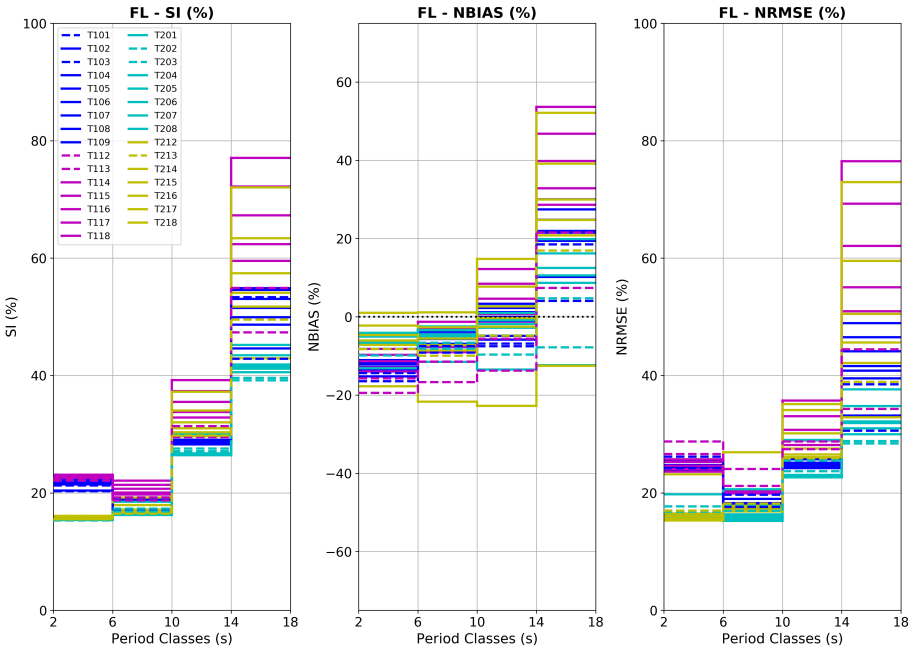

Fig. 8 Results of Hs Scatter Index (SI - left panel), Hs normalized bias (NBIAS - middle panel), and HS normalized RMSE (NRMZE - right panel) of buoy FL distributed over the classes of wave period. The dashed lines indicate the simulations with best adjustment to the observational bulk parameters: T101, T103, T112, T113, T202, T203, and T213.

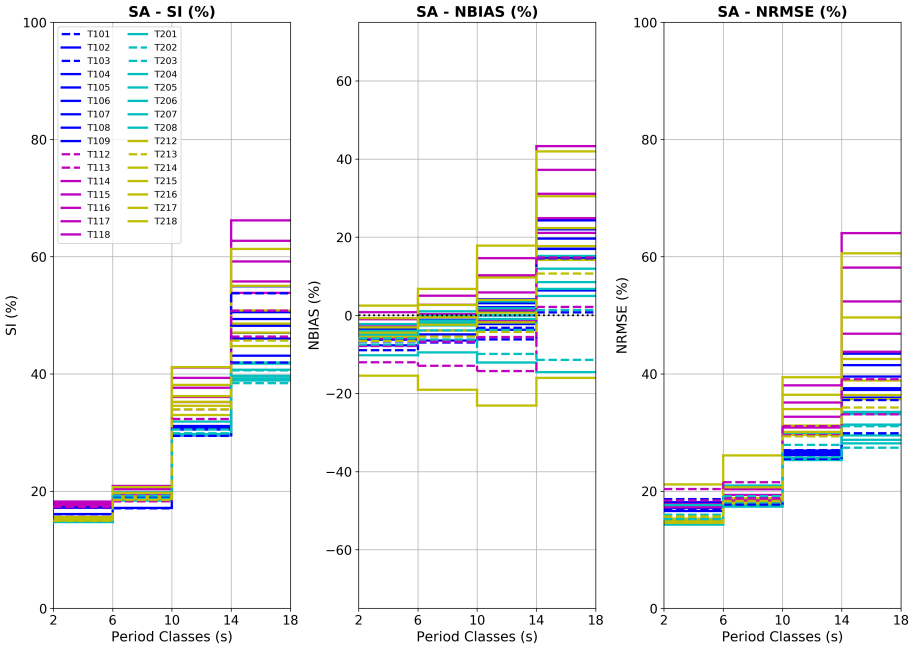

Fig. 9 Results of Hs Scatter Index (SI - left panel), Hs normalized bias (NBIAS - middle panel), and HS normalized RMSE (NRMZE - right panel) of buoy SA distributed over the classes of wave period. The dashed lines indicate the simulations with best adjustment to the observational bulk parameters: T101, T103, T112, T113, T202, T203, and T213.

7 Discussion and conclusions

This paper investigated the performance of WAVEWATCH III in the South Atlantic Ocean using two different wind inputs (NCEP/CFSR and ECMWF/ERA5), combined with two source term packages (ST4 and ST6), varying its calibration parameters β_{max} and FAC (Table 2) – a total of 31 wave hindcasts were constructed and analyzed. As the wind products have different characteristics and intensities, by adjusting the parameters β_{max} and FAC, we have shown a significantly improvement on the accuracy of wave simulations with both source terms.

The wave model responds differently according to sea state conditions and the results are influenced by both, wind input and the source term formulation. The NCEP reanalysis presents a positive bias for wind speed, in agreement with Stopa and Cheung (2014) and Campos and Guedes Soares (2016a), which is reflected on the wave fields. A positive bias of Hs has been found when considering the input from CFSR winds, i.e. the wave model tends to overestimate the observations mainly for waves with periods below 10 s. Due to stronger winds, the best error metrics and adjustments for the Q-Q plot of the wave simulations with CFSR winds are obtained with the lowest values of β_{max} and FAC, respectively 1.25 and 1.00.

In the spectral domain, the position of the analyzed points in relation to the storm areas of the South Atlantic Ocean becomes relevant in the representation of wave energy above 10 s. In this case, the choice of wind input is less important than the physical parameterization. As already shown, the results found indicate that the ST6 parameterization considerably overestimates the longer waves, so that this overestimation is greater for the RG point followed by the FL point and then SA. Considering the position of the main storm areas (Gan and Rao, 1991; Reboita et al., 2010; Gramcianinov et al., 2020a,b), the closer the analyzed point is from the storm area (but still outside of the area of influence of the storm winds), the greater the overestimation of long waves.

The recent study of Valiente et al. (2021) shows that ST4 and ST6 parameterizations present greater differences for wave growth precisely in situations of more intense winds and short fetches. Under these conditions, ST6 formulation transfers more energy from the wind to the waves and allows for faster growth of waves in the generation area. These waves disperse as they propagate beyond the generation area and then are recorded respectively by RG, FL and SA as low frequency waves. Then, the overestimation of wave energy is clearly seen in waves above 10 s, with emphasis on an overestimation of up to 80% in waves above 14 s in the simulations using ST6 parameterization for RG location.

Similarly, a recent study made by Kalourazi et al. (2021) investigated the physics sensitivity of some WAVEWATCH III parameterizations and also observed a tendency of ST6 package to present higher wave energy results due to greater transfer of energy from winds to waves. The study suggests that calibrating the coefficients that represent the effect of opposing wind (a_0) and swell dissipation (b_1) could mitigate the overestimation of wave energy by ST6 and thus improve the model performance. The calibration of these parameters and its impact on wave energy representation in the South Atlantic Ocean is not addressed by this work. However, this is a sensitive point and should be considered in future studies in order to assess possible improvements of ST6 simulations.

Therefore, a proper wave model configuration in the South Atlantic Ocean should take into account the two main characteristics: 1) the positive bias of Hs observed when using CFSR winds, which is not observed in the simulations forced by ERA5 winds, and 2) the exaggerated transfer of energy from the wind to the waves by ST6 package in the generation area that is not observed in ST4 formulation, which leads the longer waves to be better represented at RG, FL and SA points when using ST4. Finally, considering practical applications aiming for overall high performance and low systematic errors in the South Atlantic Ocean, a good choice of wave model configuration is to use the ST4 package with β_{max} between 1.55 and 1.70 and forcing winds from ERA5.

Data Availability

The wave buoys data that support the findings of this study are available in the Brazilian National Program (PNBOIA) repository (link below). The altimetry data is from Ifremer Merged Altimeter Database and it is available in CERSAT repository through the link below. The wind products (from CFSR and ERA5) are also available to the public and were derived from the following public domain resources:

PNBOIA - www.marinha.mil.br/chm/dados-do-goos-brasil/pnboia-mapa
CERSAT - http://cersat.ifremer.fr/thematic-portals/projects/globwave
CFSR - https://rda.ucar.edu/datasets/ds094.1/
ERA5 - www.ecmwf.int/en/forecasts/datasets/reanalysis-datasets/era5

References

Alves, J. H. G. d. M., Ribeiro, E. O., Matheson, G. S. G., Lima, J. A. M., and Ribeiro, C. E. P. (2009). Reconstituição do clima de ondas no sul-sudeste brasileiro entre 1997 e 2005. *Revista Brasileira de Geofísica*, 27:427 – 445.

Amante, C. and Eakins, B. (2009). Etopo1 1 arc-minute global relief model: procedures, data sources and analysis. Noaa technical memorandum, National Geophysical Data Center, NOAA.

Ardhuin, F., Chapron, B., and Collard, F. (2009). Observation of swell dissipation across oceans. *Geophysical Research Letters*, 36(6).

Ardhuin, F., Rogers, E., Babanin, A. V., Filipot, J.-F., Magne, R., Roland, A., van der Westhuysen, A., Queffeulou, P., Lefevre, J.-M., Aouf, L., and Collard, F. (2010). Semiempirical dissipation source functions for ocean waves. part i: Definition, calibration, and validation. *Journal of Physical Oceanography*, 40(9):1917–1941.

Babanin, A. V. and Jiang, H. (2017). Ocean swell: How much do we know. In *International Conference on Offshore Mechanics and Arctic Engineering*, volume 3A: Structures, Safety and Reliability of *International Conference on Offshore Mechanics and Arctic Engineering*.

Bidlot, J.-R., Janssen, P., and Abdalla, S. (2007). A revised formulation of ocean wave dissipation and its model impact. *Technical Memorandum*, page 27.

Campos, R., Alves, J., Soares, C. G., Guimaraes, L., and Parente, C. (2018). Extreme wind-wave modeling and analysis in the south atlantic ocean. *Ocean Modelling*, 124:75 – 93.

Campos, R. and Guedes Soares, C. (2016a). Comparison and assessment of three wave hindcasts in the north atlantic ocean. *Journal of Operational Oceanography*, 9:1–19.

Campos, R., Ribeiro, C., and De Camargo, R. (2012). Extreme wave analysis in campos basin (rio de janeiro - brazil) associated with extra-tropical cyclones and anticyclones. In *Proceedings of the International Conference on Offshore Mechanics and Arctic Engineering - OMAE*, volume 2.

Campos, R. M. and Guedes Soares, C. (2016b). Estimating extreme waves in brazil using regional frequency analysis. In *Proceedings of the International Conference on Offshore Mechanics and Arctic Engineering - OMAE*, volume Volume 3: Structures, Safety and Reliability.

Chawla, A., Spindler, D. M., and Tolman, H. L. (2013). Validation of a thirty year wave hindcast using the climate forecast system reanalysis winds. *Ocean Modelling*, 70:189 – 206. Ocean Surface Waves.

Cuchiara, D., Fernandes, E., Strauch, J., Winterwerp, J., and Calliari, L. (2009). Determination of the wave climate for the southern brazilian shelf. *Continental Shelf Research*, 29:545–555.

Dee, D. P., Uppala, S. M., Simmons, A. J., Berrisford, P., Poli, P., Kobayashi, S., Andrae, U., Balmaseda, M. A., Balsamo, G., Bauer, P., Bechtold, P., Beljaars, A. C. M., van de Berg, L., Bidlot, J., Bormann, N., Delsol, C., Dragani, R., Fuentes, M., Geer, A. J., Haimberger, L., Healy, S. B., Hersbach, H., Hólm, E. V., Isaksen, L., Kållberg, P., Köhler, M., Matricardi, M., McNally, A. P., Monge-Sanz, B. M., Morcrette, J.-J., Park, B.-K., Peubey, C., de Rosnay, P., Tavolato, C., Thépaut, J.-N., and Vitart, F. (2011). The era-interim reanalysis: configuration and performance of the data assimilation system. *Quarterly Journal of the Royal Meteorological Society*, 137(656):553–597.

Gan, M. A. and Rao, V. B. (1991). Surface cyclogenesis over south america. *Monthly Weather Review*, 119(5):1293 – 1302.

Godoi, V., Ribeiro, C., and Rebelo, A. (2014). An overview of events of high sea waves at the mouth of guanabara bay. *Pan-American Journal of Aquatic Sciences*, 9:70–87.

Gramcianinov, C., Campos, R., de Camargo, R., Hodges, K., Guedes Soares, C., and da Silva Dias, P. (2020a). Analysis of atlantic extratropical storm tracks characteristics in 41 years of era5 and cfsr/cfsv2 databases. *Ocean Engineering*, 216:108111.

Gramcianinov, C., Campos, R., Guedes Soares, C., and de Camargo, R. (2020b). Extreme waves generated by cyclonic winds in the western portion of the south atlantic ocean. *Ocean Engineering*, 213:107745.

Hersbach, H., Bell, B., Berrisford, P., Hirahara, S., Horányi, A., Muñoz-Sabater, J., Nicolas, J., Peubey, C., Radu, R., Schepers, D., Simmons, A., Soci, C., Abdalla, S., Abellan, X., Balsamo, G., Bechtold, P., Biavati, G., Bidlot, J., Bonavita, M., De Chiara, G., Dahlgren, P., Dee, D., Diamantakis, M., Dragani, R., Flemming, J., Forbes, R., Fuentes, M., Geer, A., Haimberger, L., Healy, S., Hogan, R. J., Hólm, E., Janisková, M., Keeley, S., Laloyaux, P., Lopez, P., Lupu, C., Radnoti, G., de Rosnay, P., Rozum, I., Vamborg, F., Villaume, S., and Thépaut, J.-N. (2020). The era5 global reanalysis. *Quarterly Journal of the Royal Meteorological*

Society, 146(730):1999–2049.

Innocentini, V., Caetano, E., and Carvalho, J. T. (2014). A procedure for operational use of wave hindcasts to identify landfall of heavy swell. *Weather and Forecasting*, 29(2):349–365.

Janssen, P. A. E. M. (1991). Quasi-linear theory of wind-wave generation applied to wave forecasting. *Journal of Physical Oceanography*, 21(11):1631–1642.

Kalnay, E., Kanamitsu, M., Kistler, R., Collins, W., Deaven, D., Gandin, L., Iredell, M., Saha, S., White, G., Woollen, J., Zhu, Y., Chelliah, M., Ebisuzaki, W., Higgins, W., Janowiak, J., Mo, K. C., Ropelewski, C., Wang, J., Leetmaa, A., Reynolds, R., Jenne, R., and Joseph, D. (1996). The ncep/ncar 40-year reanalysis project. *Bulletin of the American Meteorological Society*, 77(3):437 – 472.

Kalourazi, M. Y., Siadatmousavi, S. M., Yeganeh-Bakhtiary, A., and Jose, F. (2021). Wavewatch-iii source terms evaluation for optimizing hurricane wave modeling: A case study of hurricane ivan. *Oceanologia*, 63(2):194–213.

Kobayashi, S., Ota, Y., Harada, Y., Ebita, A., Moriya, M., Onoda, H., Onogi, K., Kamahory, H., Kobayashi, C., Endo, H., Miyaoka, K., and Takahashi, K. (2015). The jra-55 reanalysis: General specifications and basic characteristics. *Journal of the Meteorological Society of Japan. Ser. II*, 93(1):5–48.

Komen, G. J., Hasselmann, S., and Hasselmann, K. (1984). On the existence of a fully developed wind-sea spectrum. *Journal of Physical Oceanography*, 14(8):1271–1285.

Liu, Q., Rogers, W. E., Babanin, A. V., Young, I. R., Romero, L., Zieger, S., Qiao, F., and Guan, C. (2019). Observation-Based Source Terms in the Third-Generation Wave Model WAVEWATCH III: Updates and Verification. *Journal of Physical Oceanography*, 49(2):489–517.

Parente, C. E. (1999). *Uma Nova Técnica Espectral para Análise Direcional de Ondas*. PhD thesis, Federal University of Rio de Janeiro, Rio de Janeiro, RJ, Brazil.

Pereira, H. P. P., Violante-Carvalho, N., Nogueira, I. C. M., Babanin, A., Qingxiang, L., de Pinho, U. F., Nascimento, F., and Parente, C. E. (2017). Wave observations from an array of directional buoys over the southern brazilian coast. *Ocean Dynamics*, 67:1616–7228.

Pianca, C., Mazzini, P. L. F., and Siegle, E. (2010). Brazilian offshore wave climate based on nww3 reanalysis. *Brazilian Journal of Oceanography*, 58:53–70.

Queffeulou, P. and Croizé-Fillon, D. (2017). Global altimeter swh data set – version 11.4. Technical report, IFREMER.

Rapizo, H., Durrant, T., and Babanin, A. (2018). An assessment of the impact of surface currents on wave modeling in the southern ocean. *Ocean Dynamics*, 68.

Reboita, M. S., da Rocha, R. P., Ambrizzi, T., and Sugahara, S. (2010). South atlantic ocean cyclogenesis climatology simulated by regional climate model (regcm3). *Climate Dynamics*, 35:1432–0894.

Rienecker, M. M., Suarez, M. J., Gelaro, R., Todling, R., Bacmeister, J., Liu, E., Bosilovich, M. G., Schubert, S. D., Takacs, L., Kim, G.-K., Bloom, S., Chen, J., Collins, D., Conaty, A., da Silva, A., Gu, W., Joiner, J., Koster, R. D., Lucchesi, R., Molod, A., Owens, T., Pawson, S., Pegion, P., Redder, C. R., Reichle, R., Robertson, F. R., Ruddick, A. G., Sienkiewicz, M., and Woollen, J. (2011). Merra: Nasa's modern-era retrospective analysis for research and applications. *Journal of Climate*, 24(14):3624–3648.

Saha, S., Moorthi, S., Wu, X., Wang, J., Nadiga, S., Tripp, P., Behringer, D., Hou, Y.-T., Chuang, H.-y., Iredell, M., Ek, M., Meng, J., Yang, R., Mendez, M. P., van den Dool, H., Zhang, Q., Wang, W., Chen, M., and Becker, E. (2014). The ncep climate forecast system version 2. *Journal of Climate*, 27(6):2185–2208.

Semedo, A., Sušelj, K., Rutgersson, A., and Sterl, A. (2011). A global view on the wind sea and swell climate and variability from era-40. *Journal of Climate*, 24.

Stopa, J. E. (2018). Wind forcing calibration and wave hindcast comparison using multiple reanalysis and merged satellite wind datasets. *Ocean Modelling*, 127:55 – 69.

Stopa, J. E., Ardhuin, F., Babanin, A., and Zieger, S. (2016). Comparison and validation of physical wave parameterizations in spectral wave models. *Ocean Modelling*, 103:2 – 17. Waves and coastal, regional and global processes.

Stopa, J. E. and Cheung, K. F. (2014). Intercomparison of wind and wave data from the ecmwf reanalysis interim and the ncep climate forecast system reanalysis. *Ocean Modelling*, 75:65 – 83.

Tolman, H. L. and Chalikov, D. (1996). Source terms in a third-generation wind wave model. *Journal of Physical Oceanography*, 26(11):2497–2518.

Valiente, N. G., Saulter, A., Edwards, J. M., Lewis, H. W., Castillo Sanchez, J. M., Bruciaferri, D., Bunney, C., and Siddorn, J. (2021). The impact of wave model source terms and coupling strategies to rapidly developing waves across the north-west european shelf during extreme events. *Journal of Marine Science and Engineering*, 9(4).

Violante-Carvalho, N., Parente, C. E., Robinson, I. S., and Nunes, L. M. P. (2002). On the growth of wind-generated waves in a swell-dominated region in the south atlantic. *Journal of Offshore Mechanics and Arctic Engineering*, 124:14–21.

WW3DG (2019). User Manual and System Documentation of WAVEWATCH III version 6.07, The WAVEWATCH III Development Group. *Tech. Note 326 pp. + Appendices, NOAA/NWS/NCEP/MMAB*.

Young, I. R. (1999). Seasonal variability of the global ocean wind and wave climate. *International Journal of Climatology*, 19(9):931–950.

Young, I. R., Banner, M. L., Donelan, M. A., McCormick, C., Babanin, A. V., Melville, W. K., and Veron, F. (2005). An Integrated System for the Study of Wind-Wave Source Terms in Finite-Depth Water. *Journal of Atmospheric and Oceanic Technology*, 22(7):814–831.

Zieger, S., Babanin, A., Rogers, W., and Young, I. (2015). Observation-based source terms in the third-generation wave model wavewatch. *Ocean Modelling*, 96.